Omnidirectional Dual-Polarized Antenna Using Colocated Slots With Wedgy Profile

Yongjian Zhang, Peiqin Liu, *Member, IEEE*, Yuhui Yin, and Yue Li, *Senior Member, IEEE*

***Abstract*— In this article, an omnidirectional dual-polarized antenna with low windage is presented within a wedge-profiled structure for supersonic onboard systems. Based on aerodynamic analysis, a wedge-profiled cavity is designed with colocated slots for omnidirectional and dual-polarized radiation. For horizontal polarization, two identical half-wavelength slots are etched onto the cavity sidewalls symmetrically. The vertical polarization is achieved by another horizontal slot, with the port isolation higher than 42 dB. A low windage coefficient of 0.11 is obtained within the wedge-profiled cavity with the dimensions of 41.6 × 16 × 30 mm^3 (0.34λ_0 × 0.13λ_0 × 0.24λ_0). The proposed antenna is constructed and tested, with the measured results in agreement with the simulated ones. The operating bandwidths cover the band of 2.40–2.48 GHz, and the gain variations below 3.5 dB are realized in the azimuthal plane for both polarizations. The proposed wedgy antenna is with both electromagnetic and aerodynamic considerations, exhibiting the potentials in supersonic onboard communication systems.**

***Index Terms*— Antenna diversity, antenna radiation patterns, low windage, slot antennas, supersonic flight.**

I. Introduction

IN ONBOARD systems, the omnidirectional dual-polarized (ODP) antennas [1]–[4] are usually installed on the aircrafts for various applications, such as communication, positioning, and detection. For example, the ODP antennas can be used in the traffic alert and collision avoidance systems to avert collisions. There are merits of ODP antennas in practical systems. First, the antennas with omnidirectional radiation are able to provide full coverage in the azimuthal plane to improve system reliability [5]–[12]. Second, the antennas with dual polarizations are used to avoid polarization mismatching [13]–[17].

Manuscript received October 23, 2020; revised January 13, 2021; accepted February 10, 2021. Date of publication April 5, 2021; date of current version September 3, 2021. This work was supported in part by the National Natural Science Foundation of China under Grant 62022045, in part by the Youth Top Program of Beijing Outstanding Talent Funding Project, and in part by the National Key Research and Development Program of China under Grant 2018YFB1801603. *(Corresponding author: Yue Li.)*

Yongjian Zhang and Yue Li are with the Department of Electronic Engineering, Tsinghua University, Beijing 100084, China, and also with the Beijing National Research Center for Information Science and Technology, Tsinghua University, Beijing 100084, China (e-mail: lyee@tsinghua.edu.cn).

Peiqin Liu is with the Department of Electrical and Computer Engineering, National University of Singapore, Singapore 117583.

Yuhui Yin is with the School of Aerospace Engineering, Tsinghua University, Beijing 100084, China.

Color versions of one or more figures in this article are available at https://doi.org/10.1109/TAP.2021.3069517.

Digital Object Identifier 10.1109/TAP.2021.3069517

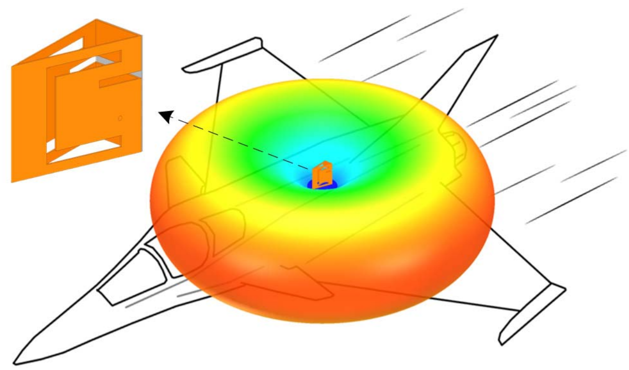

Fig. 1. General scenario of the proposed wedge-profiled ODP antenna for supersonic onboard applications.

Recently, the antennas with omnidirectional patterns have been studied with various methods. The first one is to align several identical antennas in a rotationally symmetric array configuration, providing a superimposed quasi-omnidirectional radiation pattern [18]–[20]. As another method to achieve more compact volume, the intrinsic omnidirectional antennas are developed, such as electric monopole [21], [22] or mono-cone [23], [24] antennas. The omnidirectional patterns can also be obtained using magnetic dipoles, that is, folded slots [25] and slot doublets [26]–[29]. Besides, the literatures of [30]–[33] design circular patch antennas or cavity antennas at specific operating modes for nearly omnidirectional patterns.

Next, by combining omnidirectional radiation patterns with dual-orthogonal polarizations, the ODP antennas are designed in recent works [34]–[40]. The antenna in [34] adopts a probe-fed cavity for horizontal polarization and a microstrip-fed slot for vertical polarization within a thin structure. In [35], a multiband ODP antenna is achieved by integrating a modified biconical with six printed dipoles. Soliman *et al.* [36] present a developed ODP cusp antenna with high port isolation by exciting orthogonal modes. However, as depicted in Fig. 1, the ODP antenna is usually mounted on the metal fuselage surface for onboard applications. Therefore, low windage is required for aircraft antenna design [41]–[48], especially in supersonic onboard applications. The proposed ODP antenna in [34] adopts a saber-like profile, realizing the low-windage property under low-speed airflow. In [41], an omnidirectional antenna is presented within a tapered metal cavity for supersonic platforms, but vertical polarization is not included. Up to now, it still remains a challenge to design ODP antennas with low windage for supersonic systems.

In this article, a wedge-profiled ODP antenna is proposed for low-windage supersonic applications. A slot doublet is aligned symmetrically for horizontal polarization, and a folded slot is arranged horizontally for vertical polarization. The colocated slots are all directly etched onto a thin cavity with wedgy profile for omnidirectional radiation, realizing a lower windage compared with other ODP antennas. High isolation is achieved within the structure with the dimensions of $41.6\times16\times30$ mm^3 ($0.34\lambda_0\times0.13\lambda_0\times0.24\lambda_0$, λ_0 represents the free space wavelength at 2.44 GHz). A prototype of the proposed ODP antenna is fabricated and measured. The experimental results show that azimuthal gain variations below 3.5 dB are realized in the frequency band of 2.40–2.48 GHz for dual-polarization cases. With the characteristics of low windage and high isolation, the proposed wedge-profiled ODP antenna using colocated slots has a potential for supersonic communications.

II. Low-Windage Antenna Profile

A. Antenna Profile Consideration

In onboard communication systems, it is essential to design low-windage antenna profile. Especially in supersonic systems, a shock wave occurs near the leading edge of the object, resulting in a large windage. Here, the leading edge represents the front end of the object toward the oncoming flow. Moreover, the leading edges with different shapes will occasion different types of shock waves with different values of windage, such as the normal shock wave or oblique shock wave.

Fig. 2 shows the pressure contours for different cases in the 2-D supersonic scene. The objects with different profiles are denoted by black areas. The air is assumed to be an ideal gas, and the relative velocity is 2.0 Ma (1 Ma is equal to the sound velocity). The numerical simulation is performed in the commercial software ANSYS Computational Fluid Dynamics (CFD) v16.1. As shown in Fig. 2(a), the rectangular configuration has a leading edge perpendicular to the oncoming airflow, leading to a robust normal shock wave with severe windage. Fig. 2(b) depicts a still strong oblique shock wave near the raindrop-profiled leading edge in the flow field. The wedge-profiled objects with sharp leading edges are shown in Fig. 2(c)–(e). For these wedgy cases, all airflows near the leading edges are oblique shock waves. The oblique shock wave can be divided into two types: attached oblique shock wave and detached oblique shock wave. When the wedge angle is quite small as shown in Fig. 2(c), a weak attached oblique shock wave exists near the leading edge. However, as the angle becomes larger than a certain threshold which is depended on the airflow velocity, a strong detached oblique shock wave appears as shown in Fig. 2(e), leading to a large windage coefficient. Hence, the wedgy profile with a small angle, which is involved in this work, is a competent design for low-windage supersonic applications.

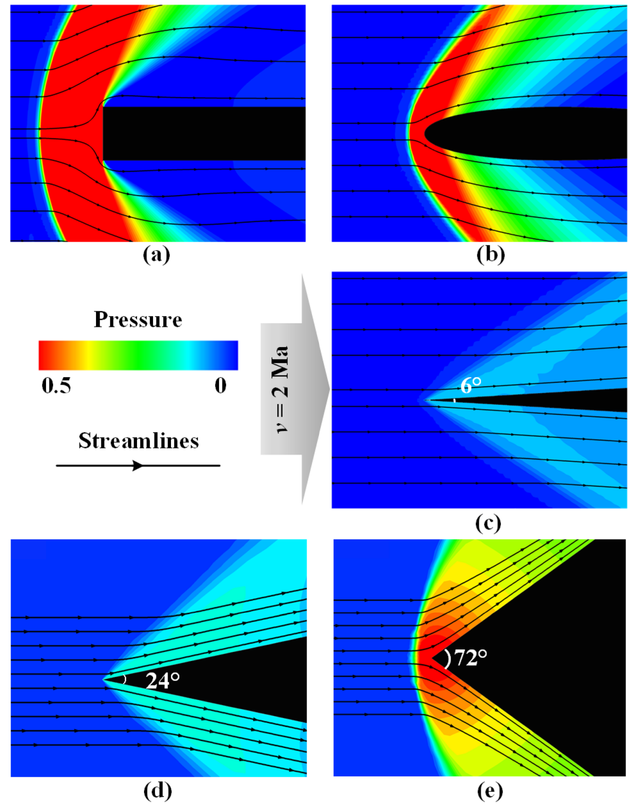

Fig. 2. Pressure contours for different cases in the 2-D supersonic scene. (a) Rectangle profile. (b) Raindrop profile. Wedge profile with different angles. (c) 6°. (d) 24°. (e) 72°.

B. Antenna Structure

Fig. 3(a) shows the geometry configuration of the proposed wedge-profiled ODP antenna, which is composed of a wedge metal cavity as the main profile and colocated slots as the radiating elements. The wedge-profiled cavity is with the sharp angle of α and the metal thickness of t_1, as shown in Fig. 3(b). The upper and lower sides of the cavity are open-ended, and other sidewalls, namely, Side 1 to Side 3, are all metal. A probe is stuck through the cavity and arranged parallel to Side 1.

Fig. 3(c) demonstrates the expanded view of the proposed antenna. Two identical C-shaped slots are etched onto Side 2 and Side 3 symmetrically. When the cavity is excited by the feeding probe through Port 1, the slot doublet operates at the half-wavelength mode, realizing a pair of in-phase equivalent magnetic currents along with the slots and omnidirectional horizontal-polarized radiation pattern in the azimuthal plane. Besides, a horizontal folded slot is carved onto three sides of the cavity, and a 50-Ω microstrip line with the F4BM dielectric ($\varepsilon_r = 2.65$) is attached on Side 1. When fed by the microstrip line through Port 2, the slot also operates at the half-wavelength mode, achieving omnidirectional vertically polarized radiation in the azimuthal plane. The total dimensions of the proposed ODP antenna are $41.6 \times 16 \times 30$ mm^3 ($0.34\lambda_0 \times 0.13\lambda_0 \times 0.24\lambda_0$). The detailed parameters are reported in Table I.

III. Antenna Design and Simulated Results

A. Slot Doublet for Horizontal Polarization

The operating principle of the proposed wedge-profiled antenna for horizontal polarization is validated by the software Ansoft HFSS 18.0. Fig. 4(a) presents the initial configuration.

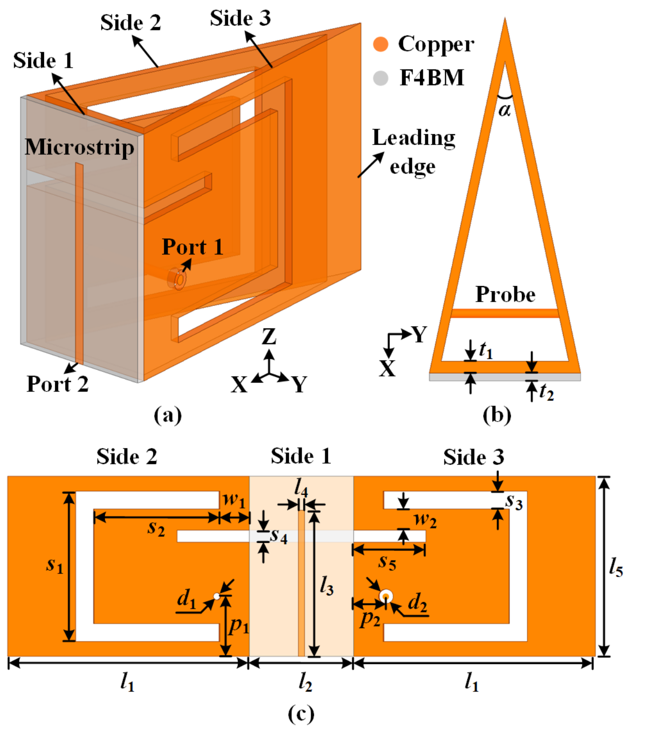

Fig. 3. Geometric configuration of the proposed antenna. (a) Perspective view. (b) Top view. (c) Expanded view.

TABLE I
DETAILED DIMENSIONS (UNIT: mm)

t_1	t_2	l_1	l_2	l_3	l_4	l_5	w_1	w_2
0.65	0.5	41.6	17.3	24.3	1	30	6.36	3.5
s_1	s_2	s_3	s_4	s_5	p_1	p_2	d_1	d_2
25	20.9	3	2	13.4	10	6	1.2	2.4

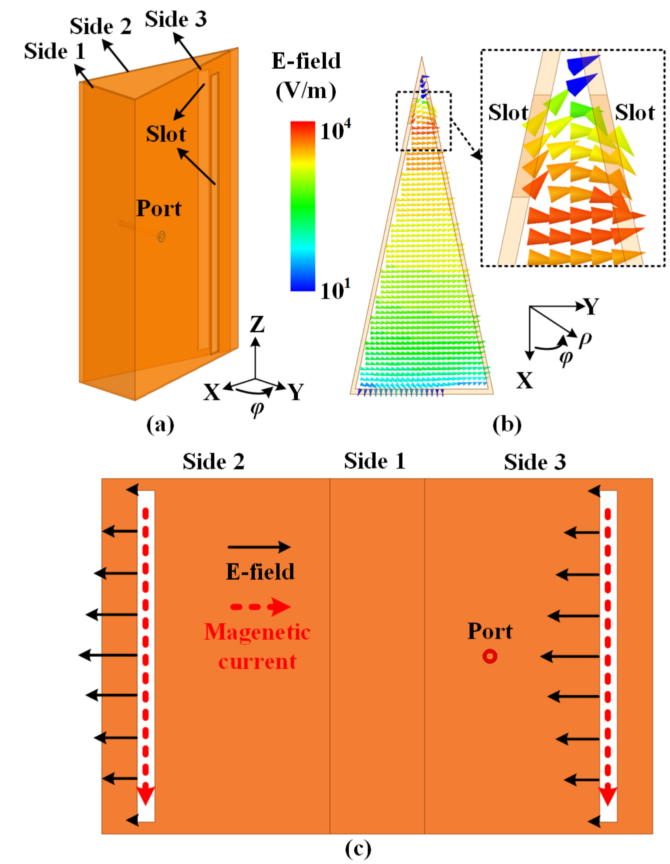

Fig. 4. Vertical straight slots for omnidirectional horizontal-polarized radiation. (a) Slot doublets carved on the wedge cavity. (b) Electric field in the cavity. (c) Magnetic currents along the slot doublet.

Based on the wedgy profile with low windage, a pair of straight slots are etched symmetrically on Side 2 and Side 3 at a proper position from the leading edge. When fed by the probe through the port, the electric field distribution on the cross section of the cavity is depicted in Fig. 4(b). In most areas away from the slots, the electric field is uniform along the φ-axis, and the null field exists on Side 1 and leading edge. Besides, large ρ components of the electric field occur near the slot doublet and out of phase on different slots, as shown in the inset of Fig. 4(b). The electric field distribution on the slot doublet is depicted in Fig. 4(c). The half-wavelength-distributed electric field on the slot doublet is denoted by black arrows. Two equivalent magnetic currents are realized in-phase along the z-axis, as denoted by red-dotted arrows. Hence, a nearly omnidirectional radiation pattern for horizontal polarization is achieved in the azimuthal plane.

B. Optimization for Low Windage

Based on the horizontal-polarized antenna configuration with the slot doublet carved onto the cavity, a series of optimization approaches to achieve lower windage coefficient are proposed under the synergetic consideration of the aerodynamic and electromagnetic characteristics. The evolution of the proposed wedge-profiled antenna is shown in Fig. 5(a)–(c). The initial antenna, named Ant. 1, is with a height larger than a half-wavelength, which is necessary due to the half-wavelength operating modes of the slot doublet. To achieve lower windage, the slot doublet is bent to C shape from Ant. 1 to Ant. 3. The whole height of the antenna is decreased gradually from 70 to 30 mm. Fig. 5(d) illustrates the radiation patterns of three antenna designs in the azimuthal plane at 2.44 GHz. It is shown that all three antennas realize omnidirectional radiation patterns in the *XOY* plane. This is because the magnetic currents on the upper and lower parts of the slot are out of phase, leading to the field cancellation in the far-field. With the decrease in the antenna height, the middle vertical part of the slot doublet is shortened, hence reducing the effective radiation aperture and decreasing the realized gain of the antenna in the azimuthal plane. Considering the tradeoff of the slot doublet length and azimuthal gain, Ant. 3 is selected for horizontal polarization, and the whole profile is with the height of $l_5 = 30$ mm.

The value of the wedge angle is also a critical part impacting on the supersonic windage. Fig. 6 and Table II illustrate the study on the influence of wedge angles on the electromagnetic and aerodynamics properties. Three antennas, named Ant. 4–Ant. 6, are with the wedge angle α which increases

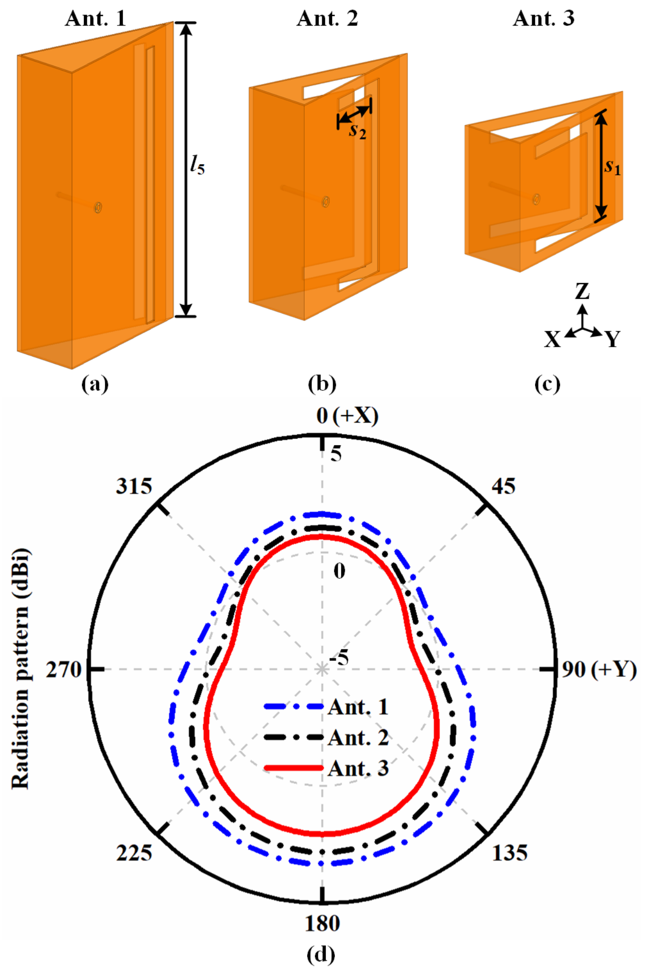

Fig. 5. Evolution of the proposed antenna for horizontal polarization. Three antennas with different profiles. (a) $l_5 = 70$ mm. $s_1 = 65$ mm. (b) $l_5 = 50$ mm. $s_1 = 45$ mm. $s_2 = 13.3$ mm. (c) $l_5 = 30$ mm. $s_1 = 25$ mm. $s_2 = 20.9$ mm. (d) Radiation patterns in the azimuthal plane at 2.44 GHz.

TABLE II

COMPARISONS AMONG THE ANTENNAS

Antenna	Gain variation (dB)	Bandwidth (MHz)	Wingdage coefficient
Ant. 4	1.27	30	0.04
Ant. 5	3.10	80	0.11
Ant. 6	5.38	110	0.21

from 12° to 36°, as shown in Fig. 6(a)–(c). Fig. 6(d) shows the radiation patterns in the *XOY* plane at 2.44 GHz. As the wedge angle increases, two equivalent magnetic currents on the slot doublet are pulled away. Hence, the antenna with the large angle achieves the larger gain variation than small ones. Besides, it is observed that Ant. 4 is with a smaller volume, leading to a higher quality factor and narrower bandwidth as illustrated in Fig. 6(e). Table II reports the windage coefficient comparison among Ant. 4–Ant. 6. Based on the aerodynamic numerical analysis, the antenna with the sharper angle has a lower windage coefficient under the supersonic airflow. As a result, considering the trade-off among the properties of gain

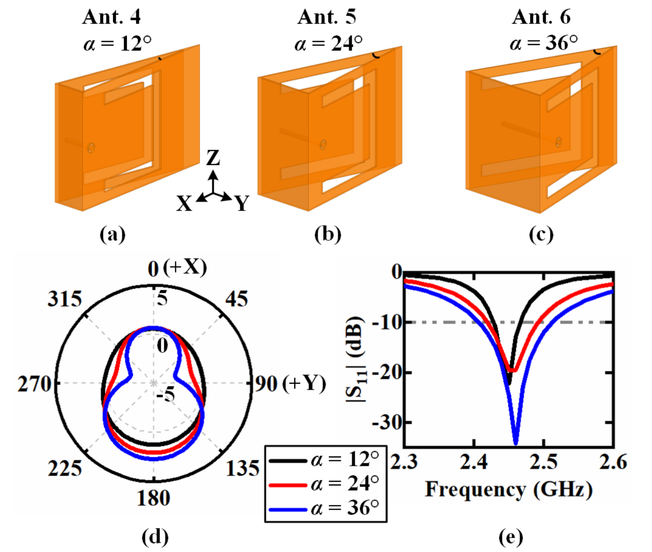

Fig. 6. Study on the influence of wedge angles on the electromagnetic properties. The antennas with different wedge angles. (a) $\alpha = 12°$. (b) $\alpha = 24°$. (c) $\alpha = 36°$. (d) Radiation patterns in the azimuthal plane at 2.44 GHz. (e) Reflection coefficients.

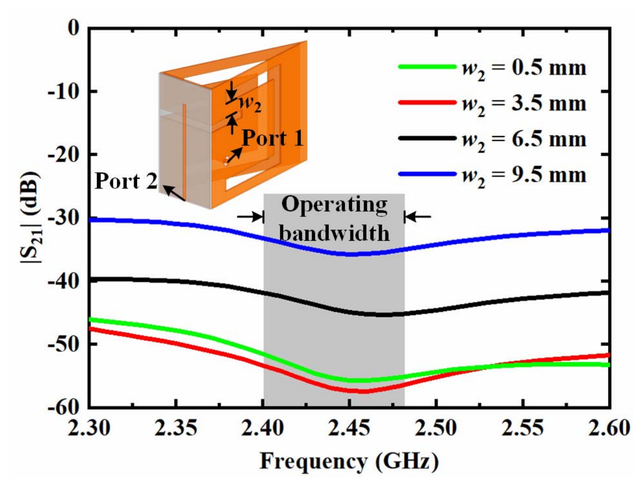

Fig. 7. Study on the influence of parameter w_2 on the port isolation.

variation, bandwidth, and windage coefficient, the optimized parameter here in this design is $\alpha = 24°$ with the windage coefficient of 0.11.

C. Dual-Polarized Configuration

Based on the wedgy profile for horizontal polarization, a folded slot is carved onto three cavity sidewalls to achieve omnidirectional vertical polarization, as shown in the inset of Fig. 7. When fed by the microstrip line through Port 2, the slot operates at the half-wavelength mode. A folded magnetic current is equivalently achieved along with the slot, radiating omnidirectional pattern in the azimuthal plane.

For ODP antenna design, the port isolation is an essential target. Owing to the orthogonal operating modes of magnetic currents for dual polarizations, high port isolation is achieved within such a compact volume. Fig. 7 illustrates the study

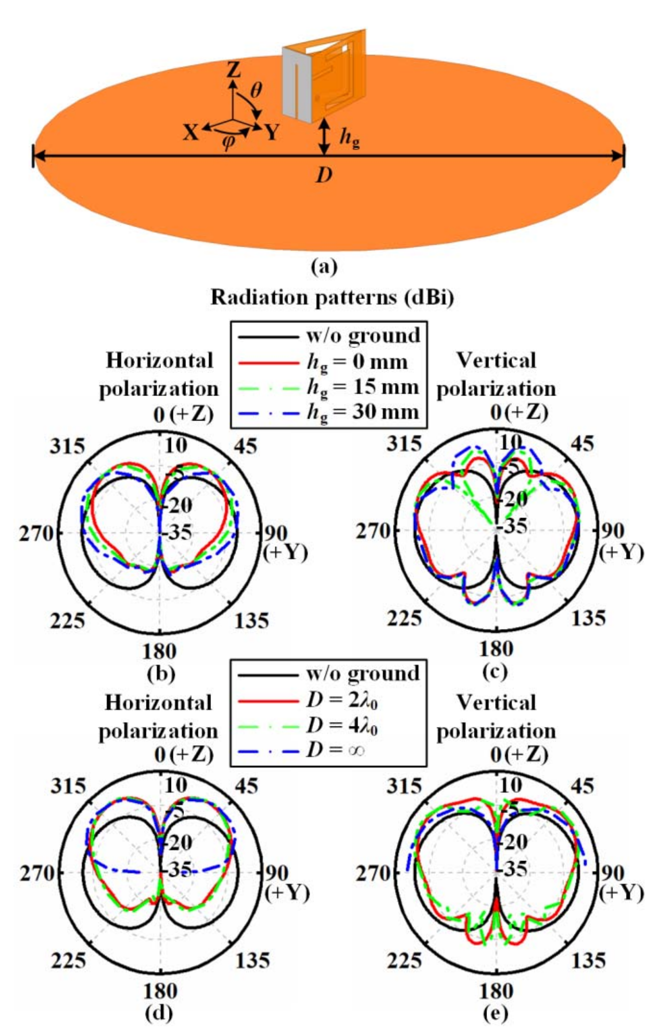

Fig. 8. Radiation properties of the proposed antenna above the metal ground. (a) Configuration. Radiation patterns in the *YOZ* plane for horizontal polarization with different values of (b) h_g and (c) D. Radiation patterns in the *YOZ* plane for vertical polarization with different values of (d) h_g and (e) D.

on the distance between colocated slots w_2 affecting the port isolation. When the horizontal slot for vertical polarization is too close to the feeding probe or the C-shaped slot doublet, the slot modes of dual-polarized radiation will be coupled, deteriorating the port isolation. Based on the parametric analysis, the distance between colocated slots is optimized as $w_2 = 3.5$ mm, with the port isolation higher than 50 dB in the band of 2.40–2.48 GHz.

D. Antenna Mounted on Ground

In the supersonic onboard systems, the ODP antennas are required for metallic fuselage installation for low windage. In this design, the ODP radiation is achieved by the colocated slots. Hence, the boundary condition of the wedge cavity has little influence on the operating modes. Fig. 8(a) depicts the antenna configuration that the proposed antenna is h_g away from the circular metal ground with the diameter of D. The metal ground has little effect on the vertically polarized radiation patterns, but it tilts up the patterns of horizontal polarization. This is because the metal ground supports the vertically polarized electromagnetic waves but not the horizontally polarized ones. Fig. 8(c) and (e) displays the copolarized radiation patterns in the *YOZ* plane for vertical polarization. It is observed that the radiation pattern remains stable with different ground sizes D or mounting distances h_g. For horizontal polarization shown in Fig. 8(b) and (d), the radiation patterns tilt upward visibly, leading to low gain in the azimuthal plane. As shown in Fig. 8(b) with $D = 2\lambda_0$, the upwarping of the radiation pattern is eased and the azimuthal gain increases by 7 dB as the mounting distance h_g varies from 0 to 30 mm. Fig. 8(d) depicts that the azimuthal gain decreases when the ground becomes larger due to the metal boundary condition. Hence, the azimuthal gain of the proposed antenna can be enhanced by modifying the ground size D or mounting distance h_g.

IV. Experimental Results

A. Antenna Fabrication

To verify the antenna design, a prototype of the proposed antenna was built and measured. The front and rear views of the fabrication are shown in Fig. 9. The fabricated prototype is composed of an all-metal cavity and a microstrip line on the substrate. As shown in the inset of Fig. 9(a), a probe protrudes into the cavity, while one end connects with the cavity sidewall. A 50-Ω semirigid coaxial cable is used to excite the cavity as port 1. The outer conductor of the cable welds to the outer surface of the cavity, and the inner conductor connects with the other end of the probe. The horizontal slot is fed through a coaxial SMA connector, with the inner conductor soldering to the fabricated microstrip line on the F4BM substrate ($\varepsilon_r = 2.65$). The S-parameters of the antenna were characterized by Agilent N9917A vector network analyzer. The radiation patterns, gain, and total efficiency were measured in a microwave anechoic chamber with a far-field antenna measurement system.

B. Antenna Measurement

The measured and simulated S-parameters are depicted in Fig. 10. The measured −10-dB impedance bandwidth is 2.40–2.48 GHz for horizontal polarization, which is close to the simulated result. For vertical polarization, the measured −10-dB bandwidth is 2.35–2.55 GHz, covering the operating bandwidth of the antenna and agreeing with the simulation. The measured transmission coefficient $|S_{21}|$ is lower than −42 dB, implying that high isolation is obtained within the wedge-profiled antenna.

Fig. 11 shows the measured and simulated radiation patterns of the proposed ODP antenna at the center frequency of 2.44 GHz for dual polarizations. It is worth mentioning that the measured radiation patterns at other frequencies in the operating bandwidth are also similar to the patterns given here. As depicted in Fig. 11(a), an omnidirectional radiation pattern is achieved in the azimuthal plane when Port 1 is excited for horizontal polarization, with the gain variation of 3.0 dB. In Fig. 11(c), the radiation pattern of vertical polarization is also omnidirectional in the azimuthal plane with

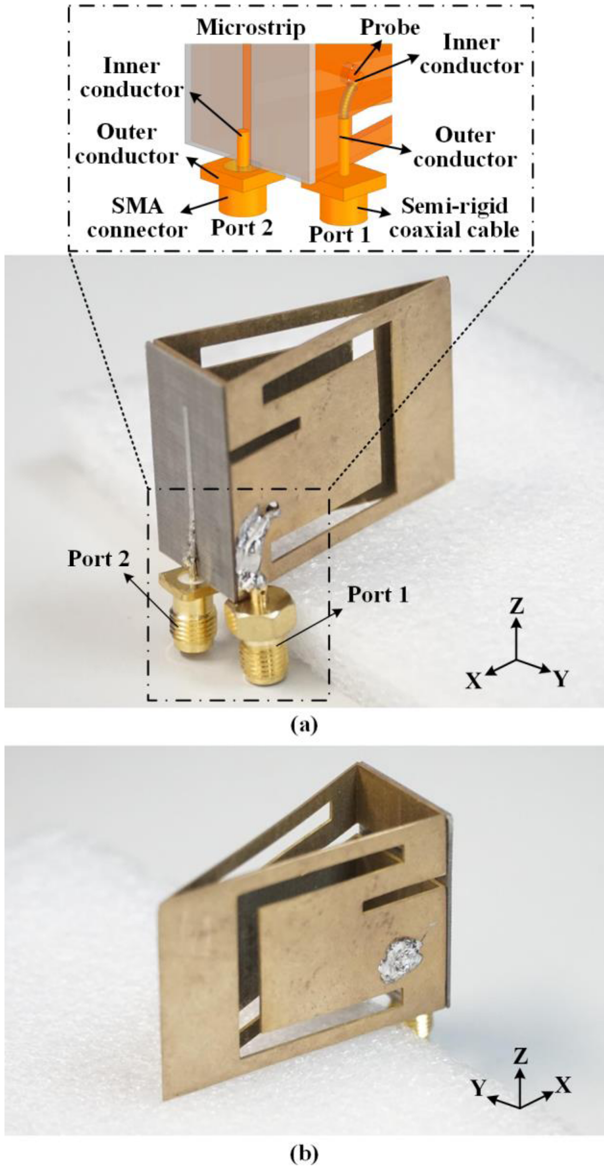

Fig. 9. Photographs of the fabricated wedge-profiled ODP antenna. (a) Front view. (b) Rear view.

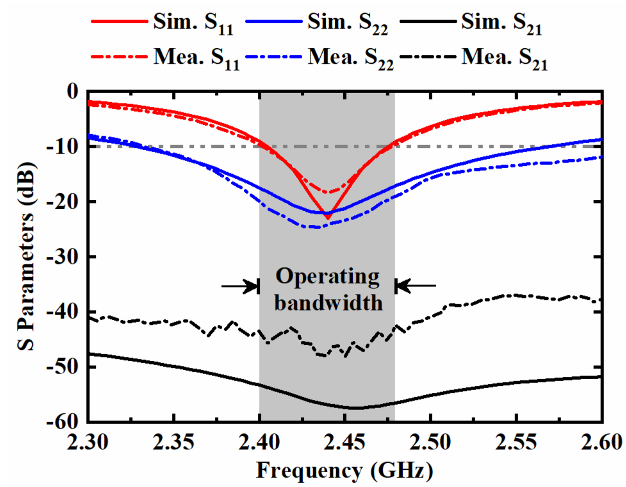

Fig. 10. Measured and simulated S-parameters of the proposed antenna.

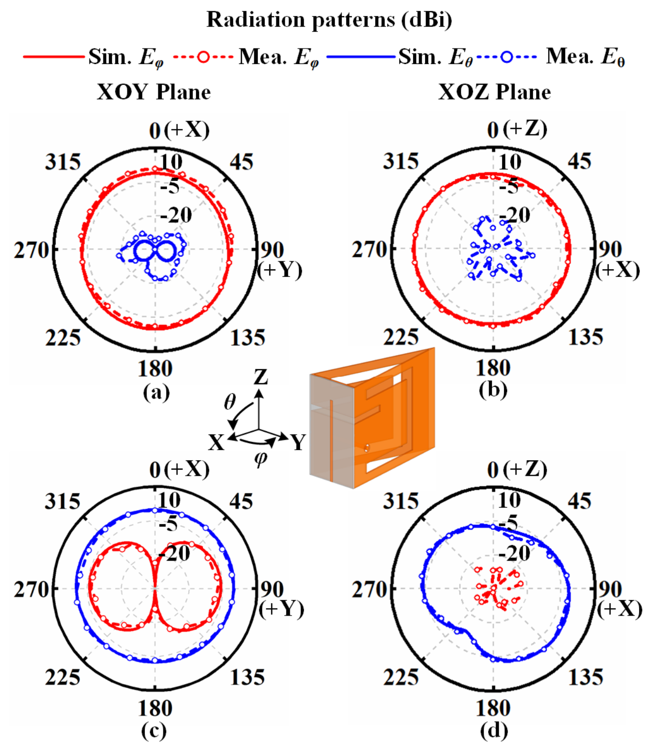

Fig. 11. Measured and simulated radiation patterns at 2.44 GHz. (a) and (b) Horizontal polarization. (c) and (d) Vertical polarization.

a gain variation of 3.5 dB. In the elevated plane, the measured copolarizations coincide well with the simulation, as shown in Fig. 11(b) and (d), which are acceptable for the ODP systems. Hence, the proposed antenna provides ODP radiation patterns in the desired frequency band of 2.40–2.48 GHz.

The simulated and measured peak realized gains and total efficiencies of the proposed ODP antenna are depicted in Fig. 12. For horizontal-polarized radiation, the measured peak realized gains are higher than 1.0 dBi in the frequency band of 2.40–2.48 GHz and reach 1.8 dBi at the center frequency of 2.44 GHz. The total efficiency higher than 80% is obtained in the proposed antenna when Port 1 is excited. The peak gain of vertical polarization is 1.4 dBi and it maintains stable gains above 1.2 dBi in the band of 2.40–2.48 GHz. While the measured total efficiency is better than 92.2% in the overall operating frequency band. The discrepancies between the measured and simulated results are mainly attributed to fabrication errors.

To highlight the performance merits of electromagnetics and aerodynamics, Table III summarizes the comparisons of the measured results in this work and other omnidirectional antenna designs for onboard systems. All these works adopt low-windage antenna structures for omnidirectional radiation, including cylinder profile [1], saber profile [25], [34], [37], and low profile [38], [49], [50]. Exactly, they are not suitable for supersonic onboard applications based on the aerodynamic analysis. Besides, due to the limit of the boundary condition,

TABLE III
COMPARISONS OF THE PROPOSED ANTENNA WITH OTHER PROTOTYPES IN THE LITERATURE

Ref.	Volume (λ_0^3)	Bandwidth (GHz)	Polarization	Gain variation (dB)	Isolation (dB)	Windage coefficient
[1]	π×0.25^2×0.67	1.70~2.30	HP / VP	1.5 / 0.5	25	N.A.
[25]	0.10×0.10×0.34	2.39~2.49	HP / VP	2.4 / 4.5	33	N.A.
[34]	0.24×0.07×0.24	2.36~2.50	HP / VP	3.2 / 4.4	20	N.A.
[37]	0.24×0.07×0.34	2.38~2.51	HP / VP	3.6 / 3.5	16	N.A.
[38]	π×0.34^2×0.23	1.70~3.90	HP / VP	N.A.	34	N.A.
[49]	π×0.15^2×0.02	1.54~1.55	CP	< 1	N.A.	N.A.
[50]	0.22×0.22×0.07	2.395~2.49	CP	0.47	N.A.	N.A.
This work	0.34×0.13×0.24	2.40-2.48	HP / VP	3.0 / 3.5	42	0.11

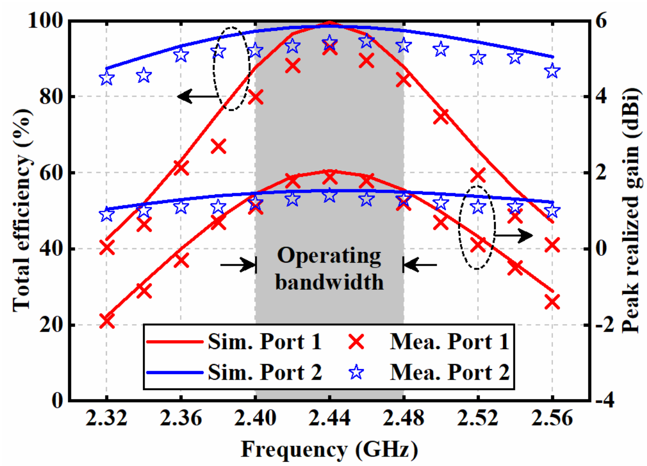

Fig. 12. Total efficiency and realized gain of the proposed antenna under simulation and measurement.

the antennas in [34] and [37] are not applicable for directly installing on the metal ground. Compared with these antenna designs, this work adopts a compact wedge-profiled structure, which is with lower windage of 0.11 in supersonic systems. Based on the electromagnetic analysis with the circular ground, the proposed antenna has the ability to install directly on the metal fuselage of the fighter, further reducing the windage of the systems. Owing to the orthogonal slot operating modes for ODP radiation, the proposed antenna obtains a higher port isolation than other reported literatures.

C. Antenna With Ground

To verify the metal-mountable antenna design, the proposed ODP antenna is directly installed on the metal circular ground with the diameter of $2\lambda_0$, as shown in Fig. 13. Fig. 13(a) depicts the photograph of the proposed antenna with the metal ground. It is worth noting that some detailed parameters in Fig. 13(b) have to be adjusted slightly for impedance matching, such as $w_1' = 10.9$ mm, $s_2' = 18.4$ mm, $s_5' = 16$ mm, and $p_2' = 3.5$ mm. The proposed antenna after modification is physically connected with the ground. Fig. 13(c) depicts the S-parameters

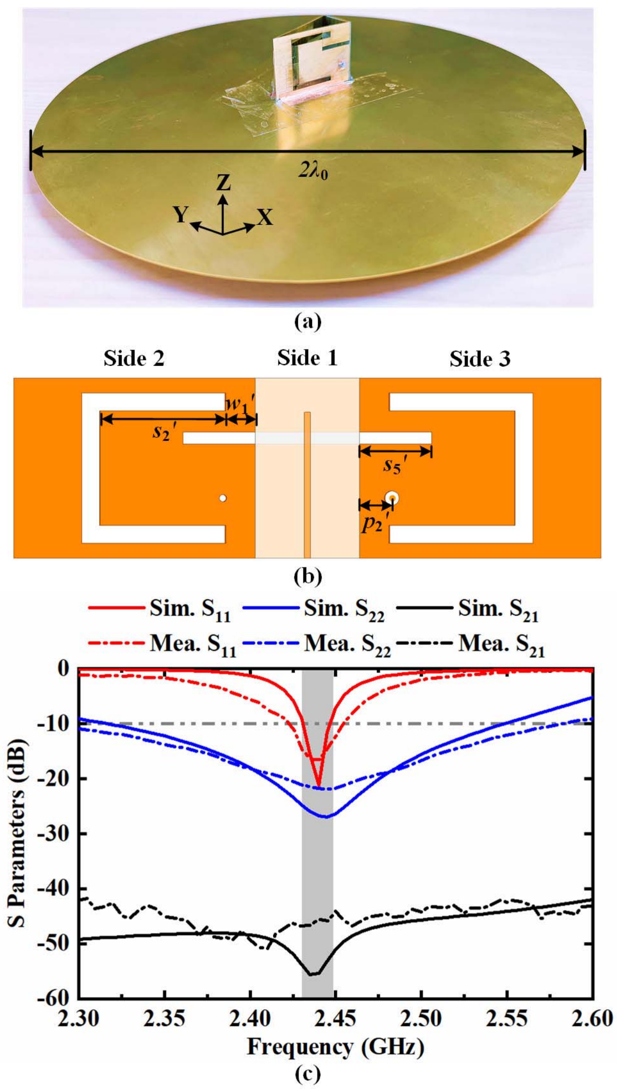

Fig. 13. Integrating the proposed antenna with the metal ground. (a) Photograph. (b) Updated dimensions of the antenna. (c) Measured and simulated S-parameters of the proposed antenna on the metal ground.

of the antenna on the circular ground. The measured results are consistent with the simulated ones. The antenna on the circular ground operates in the frequency band of 2.43–2.45 GHz for horizontal polarization, which is narrower than that of the proposed antenna without the ground. The metal boundary condition limits the operating bandwidth of the horizontal polarization. For vertical polarization, the measured -10-dB impedance bandwidth is 2.30–2.57 GHz, which is close to that without the ground. The measured transmission coefficient is below 45 dB, leading to a high port isolation in the practical applications.

V. Conclusion

In this article, an ODP antenna is proposed with wedgy profile for low-windage supersonic onboard systems. Based on the aerodynamic analysis, a wedge cavity with colocated slots is adopted as the main profile of the antenna. Two identical C-shaped slots are etched onto the wedge cavity for horizontal polarization. Meanwhile, a folded slot is carved onto three cavity sidewalls for vertical polarization. Besides, the proposed antenna can be mounted directly on the metal fuselage owing to the operating modes of the slots. The experimental results show an ODP radiation with port isolation higher than 42 dB is achieved in the desired frequency band of 2.40–2.48 GHz. With the merits of compact volume, high isolation, and low windage, the proposed wedge-profiled ODP antenna exhibits promising usage in supersonic onboard systems.

References

[1] Y. Fan, X. Liu, B. Liu, and R. Li, “A broadband dual-polarized omnidirectional antenna based on orthogonal dipoles,” *IEEE Antennas Wireless Propag. Lett.*, vol. 15, pp. 1257–1260, 2016.
[2] H. Wheeler, “Small antennas,” *IEEE Trans. Antennas Propag.*, vol. AP-23, no. 4, pp. 462–469, Jul. 1975.
[3] C. Deng, P. Li, and W. Cao, “A high-isolation dual-polarization patch antenna with omnidirectional radiation patterns,” *IEEE Antennas Wireless Propag. Lett.*, vol. 11, pp. 1273–1276, 2012.
[4] I. Ivanov, E. Levine, and H. Matzner, “Dual-polarized omni-directional antenna array based on cavity-slot elements,” in *Proc. IEEE Int. Conf. Microw. Commun. Antennas Electron. Syst.*, Nov. 2015, pp. 1–4.
[5] S. Choudhury, A. Mohan, and D. Guha, “Wideband quasi-omnidirectional planar inverted F-antenna for compact wireless systems,” *IEEE Antennas Wireless Propag. Lett.*, vol. 17, no. 7, pp. 1305–1308, Jul. 2018.
[6] S.-W. Chen, D.-Y. Wang, and W.-H. Tu, “Dual-band/tri-band/broadband CPW-fed stepped-impedance slot dipole antennas,” *IEEE Trans. Antennas Propag.*, vol. 62, no. 1, pp. 485–490, Jan. 2014.
[7] J. Oh and K. Sarabandi, “Low profile vertically polarized omnidirectional wideband antenna with capacitively coupled parasitic elements,” *IEEE Trans. Antennas Propag.*, vol. 62, no. 2, pp. 977–982, Feb. 2014.
[8] W. Hong and K. Sarabandi, “Low-profile, multi-element, miniaturized monopole antenna,” *IEEE Trans. Antennas Propag.*, vol. 57, no. 1, pp. 72–80, Jan. 2009.
[9] A. A. Omar and Z. Shen, “A compact and wideband vertically polarized monopole antenna,” *IEEE Trans. Antennas Propag.*, vol. 67, no. 1, pp. 626–631, Jan. 2019.
[10] L. Sun, Y. Li, Z. Zhang, and Z. Feng, “Compact co-horizontally polarized full-duplex antenna with omnidirectional patterns,” *IEEE Antennas Wireless Propag. Lett.*, vol. 18, no. 6, pp. 1154–1158, Jun. 2019.
[11] J. Shi, X. Wu, X. Qing, and Z. N. Chen, “An omnidirectional circularly polarized antenna array,” *IEEE Trans. Antennas Propag.*, vol. 64, no. 2, pp. 574–581, Feb. 2016.
[12] W. Hong and K. Sarabandi, “Low profile miniaturized planar antenna with omnidirectional vertically polarized radiation,” *IEEE Trans. Antennas Propag.*, vol. 56, no. 6, pp. 1533–1540, Jun. 2008.
[13] W. Sun and Y. Li, “Dual-polarized grid-slotted microstrip antenna with enhanced bandwidth and low profile,” *App. Comput. Electromagn. Soc. J.*, vol. 34, no. 3, pp. 451–456, Mar. 2019.
[14] W. Yang and Y. Pan, “A wideband dual-polarized dipole antenna with folded metallic plates,” *IEEE Antennas Wireless Propag. Lett.*, vol. 17, no. 10, pp. 1797–1801, Oct. 2018.
[15] R. Sammeta and D. S. Filipovic, “Reduced size planar dual-polarized log-periodic antenna for bidirectional high power transmit and receive applications,” *IEEE Trans. Antennas Propag.*, vol. 62, no. 11, pp. 5453–5461, Nov. 2014.
[16] E. G. Tianang, M. A. Elmansouri, and D. S. Filipovic, “Ultrawideband flush-mountable dual-polarized vivaldi antenna,” *IEEE Trans. Antennas Propag.*, vol. 68, no. 7, pp. 5670–5674, Jul. 2020.
[17] Y. Cui, Y. Niu, C. Qi, and R. Li, “A broadband flush-mountable dual-polarized dual-slot antenna,” *IEEE Antennas Wireless Propag. Lett.*, vol. 17, no. 3, pp. 501–504, Mar. 2018.
[18] A. Harmouch and H. S. A. Haddad, “Cylindrical omnidirectional slotted waveguide antenna with optimized directional characteristics,” in *Proc. 13th Medit. Microw. Symp. (MMS)*, Sep. 2013, pp. 1–4.
[19] B. Zivanovic, T. M. Weller, and C. Costas, “Series-fed microstrip antenna arrays and their application to omni-directional antennas,” *IEEE Trans. Antennas Propag.*, vol. 60, no. 10, pp. 4954–4959, Oct. 2012.
[20] G. Byun, H. Choo, and H. Ling, “Optimum placement of DF antenna elements for accurate DOA estimation in a harsh platform environment,” *IEEE Trans. Antennas Propag.*, vol. 61, no. 9, pp. 4783–4791, Sep. 2013.
[21] Q. Wu, R. Jin, J. Geng, and M. Ding, “Printed omni-directional UWB monopole antenna with very compact size,” *IEEE Trans. Antennas Propag.*, vol. 56, no. 3, pp. 896–899, Mar. 2008.
[22] A. Alipour and H. R. Hassani, “A novel omni-directional UWB monopole antenna,” *IEEE Trans. Antennas Propag.*, vol. 56, no. 12, pp. 3854–3857, Dec. 2008.
[23] M. Koohestani, J.-F. Zürcher, A. A. Moreira, and A. K. Skrivervik, “A novel, low-profile, vertically-polarized UWB antenna for WBAN,” *IEEE Trans. Antennas Propag.*, vol. 62, no. 4, pp. 1888–1894, Apr. 2014.
[24] K. Ghaemi and N. Behdad, “A low-profile, vertically polarized ultra-wideband antenna with monopole-like radiation characteristics,” *IEEE Trans. Antennas Propag.*, vol. 63, no. 8, pp. 3699–3705, Aug. 2015.
[25] Y. Li, Z. Zhang, Z. Feng, and M. F. Iskander, “Design of omnidirectional dual-polarized antenna in slender and low-profile column,” *IEEE Trans. Antennas Propag.*, vol. 62, no. 4, pp. 2323–2326, Apr. 2014.
[26] A. J. Sangster and H. Wang, “Resonance properties of omnidirectional slot doublet in rectangular waveguide,” *Electron. Lett.*, vol. 29, no. 1, pp. 16, Jan. 1993.
[27] J.-Y. Li and L.-W. Li, “Analysis of omnidirectional waveguide slots array antennas,” in *Proc. 6th Int. Symp. Antennas, Propag. EM Theory*, 2003, pp. 38–41.
[28] R. K. Gayen and S. Das, “Design and analysis of waveguide slot doublets for dual band or nearly–omnidirectional radiation properties,” in *Proc. IEEE-APS Topical Conf. Antennas Propag. Wireless Commun. (APWC)*, Sep. 2012, pp. 522–525.
[29] H. R. Jha and S. N. Singh, “Design and analysis of waveguide-fed broad-wall longitudinal log periodic slotted array antenna for 8.2~11.11 GHz frequency applications,” *Int. J. Adv. Eng. Res. Sci.*, vol. 1, no. 6, pp. 15–24, Nov. 2014.
[30] Z.-G. Liu and Y.-X. Guo, “Dual band low profile antenna for body centric communications with a split ring resonator,” in *IEEE MTT-S Int. Microw. Symp. Dig.*, Dec. 2013, pp. 1–3.
[31] J. Liu, Q. Xue, H. Wong, H. W. Lai, and Y. Long, “Design and analysis of a low-profile and broadband microstrip monopolar patch antenna,” *IEEE Trans. Antennas Propag.*, vol. 61, no. 1, pp. 11–18, Jan. 2013.
[32] Y.-M. Cai, S. Gao, Y. Yin, W. Li, and Q. Luo, “Compact-size low-profile wideband circularly polarized omnidirectional patch antenna with reconfigurable polarizations,” *IEEE Trans. Antennas Propag.*, vol. 64, no. 5, pp. 2016–2021, May 2016.
[33] Y. Li, Z. Zhang, and Z. Feng, “Magnetic current synthesis using cavity structures,” in *Proc. 32nd Gen. Assem. Sci. Symp. Int. Union Radio Sci. (URSI GASS)*, Aug. 2017, pp. 1–4.
[34] P. Liu, Z. Meng, L. Wang, Y. Zhang, and Y. Li, “Omnidirectional dual-polarized saber antenna with low wind drag,” *IEEE Trans. Antennas Propag.*, vol. 68, no. 1, pp. 558–563, Jan. 2020.
[35] X.-W. Dai, Z.-Y. Wang, C.-H. Liang, X. Chen, and L.-T. Wang, “Multi-band and dual-polarized omnidirectional antenna for 2G/3G/LTE application,” *IEEE Antennas Wireless Propag. Lett.*, vol. 12, pp. 1492–1495, Nov. 2013.
[36] E. A. Soliman, M. S. Ibrahim, and A. K. Abdelmageed, “Dual-polarized omnidirectional planar slot antenna for WLAN applications,” *IEEE Trans. Antennas Propag.*, vol. 53, no. 9, pp. 3093–3097, Sep. 2005.

[37] P. Liu, Y. Li, Z. Zhang, and Z. Feng, "Omnidirectional dual-polarized antenna with sabre-like structure," *IEEE Trans. Antennas Propag.*, vol. 65, no. 6, pp. 3221–3225, Jun. 2017.

[38] S. X. Ta, D. M. Nguyen, K. K. Nguyen, C. Dao-Ngoc, and N. Nguyen-Trong, "Dual-polarized omnidirectional antenna with simple feed and ultrawide bandwidth," *IEEE Antennas Wireless Propag. Lett.*, vol. 19, no. 5, pp. 871–875, May 2020.

[39] Y. Liu, X. Li, L. Yang, and Y. Liu, "A dual-polarized dual-band antenna with omni-directional radiation patterns," *IEEE Trans. Antennas Propag.*, vol. 65, no. 8, pp. 4259–4262, Aug. 2017.

[40] Q. Gong, R. L. Li, and Y. Cui, "Tri-band dual-polarised omnidirectional antenna with high isolation for unmanned aerial vehicle applications," *Electron. Lett.*, vol. 54, no. 18, pp. 1059–1060, Sep. 2018.

[41] H. Nawaz, X. Liang, M. S. Sadiq, and M. A. B. Abbasi, "Ruggedized surface-mount omnidirectional antenna for supersonic aerial platforms," *IEEE Antennas Wireless Propag. Lett.*, vol. 19, no. 8, pp. 1439–1442, Aug. 2020.

[42] X. Chen, L. Yang, J.-Y. Zhao, and G. Fu, "High-efficiency compact circularly polarized microstrip antenna with wide beamwidth for airborne communication," *IEEE Antennas Wireless Propag. Lett.*, vol. 15, pp. 1518–1521, Jan. 2016.

[43] S. Kemkemian, I. L. Roy-Naneix, S. Mallegol, B. Perpère, and C. Renard, "Wideband and very wideband thin structural tiles for airborne active antennas," in *Proc. Eur. Conf. Antennas Propag.*, Apr. 2013, pp. 2744–2747.

[44] M. Nosrati, A. Jafargholi, R. Pazoki, and N. Tavassolian, "Broadband slotted blade dipole antenna for airborne UAV applications," *IEEE Trans. Antennas Propag.*, vol. 66, no. 8, pp. 3857–3864, Aug. 2018.

[45] C. Y. Rhee, J. H. Kim, W. J. Jung, T. Park, B. Lee, and C. W. Jung, "Frequency-reconfigurable antenna for broadband airborne applications," *IEEE Antennas Wireless Propag. Lett.*, vol. 13, pp. 189–192, Jan. 2014.

[46] S. P. Singh, A. Kumar, V. K. Singh, and Sagar, "A broadband wide beamwidth circulary polarized microstrip patch antenna with conformal radome for high-speed airborne communication," in *Proc. Int. Conf. Innov. Electron., Signal Process. Commun. (IESC)*, Apr. 2017, pp. 155–158.

[47] G. Byun, C. Seo, B.-J. Jang, and H. Choo, "Design of aircraft on-glass antennas using a coupled feed structure," *IEEE Trans. Antennas Propag.*, vol. 60, no. 4, pp. 2088–2093, Apr. 2012.

[48] L. Rufail and J.-J. Laurin, "Aircraft cavity-backed nonprotruding wideband antenna," *IEEE Antennas Wireless Propag. Lett.*, vol. 11, pp. 1108–1111, Sep. 2012.

[49] L. Peng, K. Sun, X. Jiang, S.-M. Li, and C.-L. Ruan, "EZR-MZR resonators for compact low-profile omnidirectional circular-polarized antenna design," *IEEE Photon. J.*, vol. 9, no. 4, pp. 1–15, Aug. 2017.

[50] Y. Yu, Z. Shen, and S. He, "Compact omnidirectional antenna of circular polarization," *IEEE Antennas Wireless Propag. Lett.*, vol. 11, pp. 1466–1469, 2012.

Yongjian Zhang received the B.S. degree in communication engineering from Tongji University, Shanghai, China, in 2018. He is currently pursuing the Ph.D. degree in electronic engineering from Tsinghua University, Beijing, China.

His current research interests include aircraft antennas, dual-polarized antennas, and multiple-input and multiple-output (MIMO) antenna arrays. He serves as a Reviewer for the IEEE TRANSACTIONS ON ANTENNAS AND PROPAGATION, IEEE ANTENNAS AND WIRELESS PROPAGATION LETTERS, and *Microwave and Optical Technology Letters*.

Peiqin Liu (Member, IEEE) received the B.S. degree from the University of Electronic Science and Technology of China, Chengdu, China, in 2014, and the Ph.D. degree in electronic engineering from Tsinghua University, Beijing, China, in 2019.

Since September 2019, he has been with the National University of Singapore, Singapore, where he is currently a Research Fellow. His current research interests include metamaterial and antenna theory, particularly in novel metasurface with artificial intelligence methods. He has authored or coauthored more than 20 technical articles published in international journals and conferences and holds five granted Chinese patents.

Dr. Liu was a recipient of the Third Prize of the Best Student Paper Award of 2017 Asia-Pacific Conference on Antennas and Propagation (APCAP), the Best Student Paper Award of 2017 National Conference on Antennas (NCANT), and the Outstanding Student Paper Award of 2018 Cross Strait Quad-Regional Radio Science and Wireless Technology Conference (CSQRWC).

Yuhui Yin received the B.S. degree in engineering mechanics from Tsinghua University, Beijing, China, in 2017. He is currently pursuing the Ph.D. degree in aeronautical and astronautical science and technology from Tsinghua University, Beijing, China.

His current research interests include the computational fluid dynamics and turbulence modeling.

Yue Li (Senior Member, IEEE) received the B.S. degree in telecommunication engineering from Zhejiang University, Zhejiang, China, in 2007, and the Ph.D. degree in electronic engineering from Tsinghua University, Beijing, China, in 2012.

He is currently an Associate Professor with the Department of Electronic Engineering with Tsinghua University. In June 2012, he was a Postdoctoral Fellow with the Department of Electronic Engineering, Tsinghua University. In December 2013, he was a Research Scholar with the Department of Electrical and Systems Engineering, University of Pennsylvania, Philadelphia, PA, USA. He was also a Visiting Scholar with the Institute for Infocomm Research (I2R), A∗STAR, Singapore, in 2010, and Hawaii Center of Advanced Communication (HCAC), University of Hawaii at Manoa, Honolulu, HI, USA, in 2012. Since January 2016, he has been with Tsinghua University, where he is currently an Assistant Professor. He has authored or coauthored over 150 journal articles and 45 international conference papers, and holds 23 granted Chinese patents. His current research interests include metamaterials, plasmonics, electromagnetics, nanocircuits, mobile and handset antennas, MIMO and diversity antennas, and millimeter-wave antennas and arrays.

He was a recipient of the Issac Koga Gold Medal from URSI General Assembly in 2017, the Second Prize of Science and Technology Award of China Institute of Communications in 2017, the Young Scientist Awards from the conferences of Progress In Electromagnetics Research Symposium (PIERS) 2019, International Applied Computational Electromagnetics Society Symposium (ACES) 2018, Atlantic Radio Science Conference (AT-RASC) 2018, Asia–Pacific Radio Science Conference (AP-RASC) 2016, International Symposium on Electromagnetic Theory (EMTS) 2016, URSI General Assembly and Scientific Symposium (GASS) 2014, the Best Paper Awards from the conferences of International Symposium on Antennas and Propagation (ISAP) 2019, Cross Strait Quad-Regional Radio Science and Wireless Technology Conference (CSQRWC) 2018, National Conference on Microwave and Millimeter Waves (NCMMW) 2018 and 2017, Asia–Pacific Conference on Antennas and Propagation (APCAP) 2017, National Conference on Antennas (NCANT) 2019 and 2017, International Symposium on Antennas, Propagation and EM Theory (ISAPE) 2016, and International Conference on Microwave and Millimeter Wave Technology (ICMMT) 2016, the Outstanding Doctoral Dissertation of Beijing Municipality in 2013, and the Principal Scholarship of Tsinghua University in 2011. He is serving as the Associate Editor of IEEE TRANSACTIONS ON ANTENNAS AND PROPAGATION, IEEE ANTENNAS AND WIRELESS PROPAGATION LETTERS, *Microwave and Optical Technology Letters*, and *Computer Applications in Engineering Education*, also as the Editorial Board of *Scientific Report*.